Image Reconstruction from Readout-Multiplexed Single-Photon Detector Arrays

Supplementary Material

1. Bias Calculations

As noted in Fig. 1 and Sec. 4 of the main paper, the single-photon estimator is unbiased and the naive estimator has a positive bias. Here, we analytically derive these results.

1.1. Naive Estimator

For a given readout frame (R^t, C^t), the naive estimator imputes a photon count to pixel (i,j) when there is a detection at (i,j) (with probability q_{ij}) or when detections occur in row i and column j, but not at pixel (i,j). The probability of the latter is

$$(1-q_{ij})\left(1-\prod_{k\in R_i'}(1-q_{kj})\right)\left(1-\prod_{\ell\in C_j'}(1-q_{i\ell})\right),$$

where R_i' and C_j' are the sets of rows and columns excluding row i and column j, respectively. Then $R_i^t C_j^t \sim \text{Bernoulli}(q_{ij}')$, where

$$\begin{aligned} q_{ij}' =& q_{ij} + (1-q_{ij}) \\ & \left(1-\prod_{k\in R_i'}(1-q_{kj})\right)\left(1-\prod_{\ell\in C_j'}(1-q_{i\ell})\right). \end{aligned} \tag{17}$$

Therefore, the bias of the naive estimator is

$$\begin{aligned} &\mathbb{E}[\widehat{q}_{ij,\text{naive}}] - q_{ij} \\ &= (1-q_{ij})\left(1-\prod_{k\in R_i'}(1-q_{kj})\right)\left(1-\prod_{\ell\in C_j'}(1-q_{i\ell})\right). \end{aligned} \tag{18}$$

1.2. Single-Photon Estimator

As defined in (7), the single-photon estimator is $N_{ij}/(N_{ij}+N_0)$ if $N_{ij}+N_0>0$ and 0 otherwise. Here, N_{ij} is the number of frames with a single detected photon at pixel (i,j), and N_0 is the number of frames with no detected photons at the array. We show this estimator to be unbiased when $N_{ij}+N_0>0$. The expected value of the estimate is

$$\begin{aligned} \mathbb{E}\left[\widehat{q}_{ij,\text{single}}\right] &\overset{(a)}{=} \mathbb{E}\left[\mathbb{E}\left[\frac{N_{ij}}{N_{ij}+N_0}\middle| N_{ij}+N_0\right]\right] \\ &= \mathbb{E}\left[\frac{\mathbb{E}\left[N_{ij}|N_{ij}+N_0\right]}{N_{ij}+N_0}\right] \\ &\overset{(b)}{=} \mathbb{E}\left[\frac{q_{ij}(N_{ij}+N_0)}{N_{ij}+N_0}\right] \\ &= q_{ij}, \end{aligned}$$

where (a) follows from the law of iterated expectation and (b) follows from the fact that $N_{ij}\,|\,(N_{ij}+N_0) \sim \text{Binomial}(R_{ij}/(R_0+R_{ij}), N_{ij}+N_0)$ with

$$\begin{aligned} R_0 &= \prod_{k=1}^{n}\prod_{\ell=1}^{n}(1-q_{k\ell}), \\ R_{ij} &= q_{ij}\prod_{k=1,\ell=1,(k,\ell)\neq(i,j)}^{k=n,\ell=n}(1-q_{k\ell}). \end{aligned}$$

2. General Form of the Multiphoton Estimator

The likelihood of all photon incidence frames $\{Y^t\}_{t=1}^T$ is

$$\mathcal{L}(q;\{Y^t\}_{t=1}^T) = \prod_{t=1}^{T} p_Y(Y^t;q), \tag{19}$$

where

$$p_Y(y;q) = \prod_{i=1}^{m}\prod_{j=1}^{n} q_{ij}^{y_{ij}}(1-q_{ij})^{1-y_{ij}} \tag{20}$$

is the probability mass function (PMF) of a photon incidence indicator. If we observe $\{Y^t\}_{t=1}^T$, then the maximum likelihood estimator of q is

$$\widehat{q}_{ij} = \frac{1}{T}\sum_{t=1}^{T} Y_{ij}^t. \tag{21}$$

With row–column readouts $\{(R^t,C^t)\}_{t=1}^T$, a frame may be ambiguous, i.e., a readout (R^t,C^t) can arise from many possible photon incidence events. Let $\boldsymbol{A}:(R^t,C^t)\mapsto\mathcal{Y}^t$ be a mapping from a row–column readout to a set of possible photon incidence indicators. For example, in a 2×2 detector array,

$$\boldsymbol{A}\left(\begin{bmatrix}1\\1\end{bmatrix},\begin{bmatrix}1\\1\end{bmatrix}\right) = \left\{\begin{bmatrix}1&0\\0&1\end{bmatrix},\ \begin{bmatrix}0&1\\1&0\end{bmatrix},\ \begin{bmatrix}1&1\\0&1\end{bmatrix},\ \begin{bmatrix}1&1\\1&0\end{bmatrix},\ \begin{bmatrix}1&0\\1&1\end{bmatrix},\ \begin{bmatrix}0&1\\1&1\end{bmatrix},\ \begin{bmatrix}1&1\\1&1\end{bmatrix}\right\}, \tag{22}$$

as illustrated in Fig. 2. The probability of a readout (R^t,C^t) is the sum of the probabilities of all possible photon incidence indicators. The PMF of a readout is

$$p_{R,C}(r,c;q) = \sum_{Y\in\boldsymbol{A}(r,c)} p_Y(Y;q). \tag{23}$$

The likelihood of all row–column readout frames is

$$\mathcal{L}(q; \{(R^t, C^t)\}_{t=1}^T) = \prod_{t=1}^T p_{R,C}(R^t, C^t; q). \quad (24)$$

Maximizing the likelihood (24) is computationally difficult because the ambiguous frames render the log likelihood nonconcave with respect to q. Instead of maximizing the photon incidence likelihood (24), the ME maximizes its approximation by distributing each ambiguous readout to possible photon incidence events according to $\widehat{q}_{\text{single}}$. Let the approximate likelihood be

$$\widetilde{\mathcal{L}}(q; \{(R^t, C^t)\}_{t=1}^T) = \prod_{t=1}^T \widetilde{p}_{R,C}(R^t, C^t; q), \quad (25)$$

where

$$\widetilde{p}_{R,C}(r, c; q) = \prod_{Y \in \boldsymbol{A}(r,c)} p_Y(g(Y, \boldsymbol{A}(r,c))Y; q) \quad (26)$$

and

$$g(Y, \boldsymbol{A}(r,c)) = \frac{p_Y(Y; \widehat{q}_{\text{single}})}{\sum_{Y' \in \boldsymbol{A}(r,c)} p_Y(Y'; \widehat{q}_{\text{single}})} \quad (27)$$

approximates the probability of Y given a row–column readout (r, c). For example, in a 2×2 array as demonstrated in Fig. 2, there is only one type of ambiguous readout with $R^t = [1, 1]$ and $C^t = [1, 1]$ corresponding to events $E_9, \ldots, E_{15}$. Maximizing the approximate likelihood (25) becomes similar to estimating q from the photon incidence indicators $\{Y^t\}_{t=1}^T$ as in (21). The ME is therefore

$$\widehat{q}_{ij,\text{multi}} = \frac{1}{T} \sum_{t=1}^T \sum_{Y \in \boldsymbol{A}(R^t, C^t)} g(Y, \boldsymbol{A}(R^t, C^t)) Y_{ij}. \quad (28)$$

Intuitively, the ME estimates q from a dataset of photon incidence indicators $\cup_{t=1}^T \boldsymbol{A}(R^t, C^t)$ synthesized from possibly ambiguous row–column readouts $\{(R^t, C^t)\}_{t=1}^T$. In the estimator, each synthesized photon incidence indicator $Y \in \boldsymbol{A}(R^t, C^t)$ is weighted according to the probability that it arises from the readout (R^t, C^t) according to a preliminary estimate $\widehat{q}_{\text{single}}$.

3. Bias–Variance Decomposition of MSE

Fig. 4 shows the MSE as a function of mean PPF of the naive, single-, and multiphoton estimators. To better understand their behaviors, here we study the explicit change of bias and variance of each of the estimators as functions of mean PPF. Fig. 9(a) shows that the bias of the SPE is 0 across the range of PPF values, while the naive estimator has a large positive bias. The multiphoton estimator has a small negative bias that decreases as the number of photons

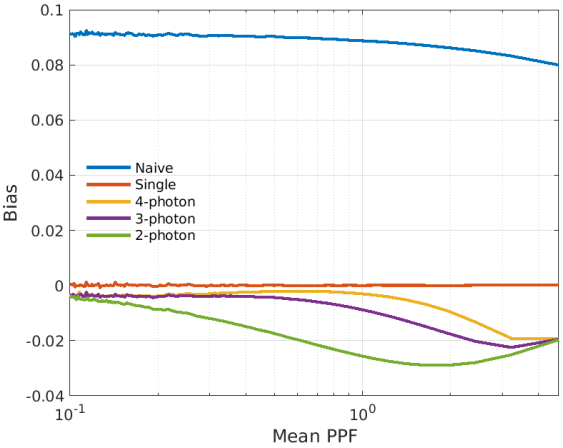

(a) Bias

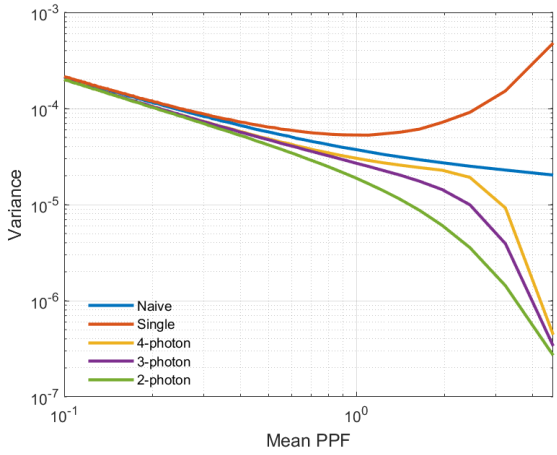

(b) Variance

Figure 9. Change in bias and variance of the naive, single-photon, and multiphoton estimators as functions of mean photons per frame.

modeled by the estimator increases. This negative bias is due to the multiphoton estimator imputing at most 4 coincident photons to ambiguous readouts that may have been produced by more coincident photons. Fig. 9(b) shows that the variance of the SPE is high, especially at high incident photon fluxes. This is expected since the SPE discards all ambiguous readouts, which have high probabilities of occurrence in the high incident flux cases. The ME achieves the lowest variance of the three estimators.

4. Fisher Information Matrix Calculation

The Cramér–Rao bound in Fig. 7 is obtained by averaging over the diagonal elements of the inverse of the Fisher information matrix, which is derived using the log-likelihood expression for row–column readouts. Here, we provide an

explicit derivation of the entries in the FIM for a 2×2 array.

The number of readout frames of each type $M_0, \ldots, M_9$ can be modeled as

$$(M_0, M_1, \ldots, M_9) \sim \text{Multinomial}(r_0, r_1, \ldots, r_9, T), \tag{29}$$

where T is the number of measured frames and $r_0, \ldots, r_9$ are the probabilities of events $E_0, \ldots, E_9$ given by

$$\begin{aligned} r_0 &= (1-q_{11})(1-q_{12})(1-q_{21})(1-q_{22}), \\ r_1 &= (q_{11})(1-q_{12})(1-q_{21})(1-q_{22}), \\ r_2 &= (q_{12})(1-q_{11})(1-q_{21})(1-q_{22}), \quad \ldots, \\ r_9 &= (q_{11}q_{22} + q_{12}q_{21} - q_{11}q_{12}q_{21}q_{22}). \end{aligned} \tag{30}$$

Further, for a 2×2 array, the expressions for v_{ij} and f_{ij} in the likelihood expression (10) are

$$\begin{aligned} v_{11} &= M_0 + M_2 + M_3 + M_4 + M_7 + M_8, \\ f_{11} &= M_1 + M_5 + M_6, \\ v_{12} &= M_0 + M_1 + M_3 + M_4 + M_6 + M_8, \\ f_{12} &= M_2 + M_5 + M_7, \\ v_{21} &= M_0 + M_1 + M_2 + M_4 + M_5 + M_7, \\ f_{21} &= M_3 + M_6 + M_8, \\ v_{22} &= M_0 + M_1 + M_2 + M_3 + M_5 + M_6, \\ f_{22} &= M_4 + M_7 + M_8. \end{aligned} \tag{31}$$

The Fisher information matrix of size 4×4 is then calculated as

$$\mathcal{I} = -\mathbb{E}\begin{bmatrix} \frac{\partial^2 \mathcal{L}'}{\partial q_{11}^2} & \frac{\partial^2 \mathcal{L}'}{\partial q_{11}\partial q_{12}} & \frac{\partial^2 \mathcal{L}'}{\partial q_{11}\partial q_{21}} & \frac{\partial^2 \mathcal{L}'}{\partial q_{11}\partial q_{22}} \\ \frac{\partial^2 \mathcal{L}'}{\partial q_{12}\partial q_{11}} & \frac{\partial^2 \mathcal{L}'}{\partial q_{12}^2} & \frac{\partial^2 \mathcal{L}'}{\partial q_{12}\partial q_{21}} & \frac{\partial^2 \mathcal{L}'}{\partial q_{12}\partial q_{22}} \\ \frac{\partial^2 \mathcal{L}'}{\partial q_{21}\partial q_{11}} & \frac{\partial^2 \mathcal{L}'}{\partial q_{21}\partial q_{12}} & \frac{\partial^2 \mathcal{L}'}{\partial q_{21}^2} & \frac{\partial^2 \mathcal{L}'}{\partial q_{21}\partial q_{22}} \\ \frac{\partial^2 \mathcal{L}'}{\partial q_{22}\partial q_{11}} & \frac{\partial^2 \mathcal{L}'}{\partial q_{22}\partial q_{12}} & \frac{\partial^2 \mathcal{L}'}{\partial q_{22}\partial q_{21}} & \frac{\partial^2 \mathcal{L}'}{\partial q_{22}^2} \end{bmatrix}, \tag{32}$$

where $\mathcal{L}' = \log(\mathcal{L})$. Consider $\mathcal{I}_{11}$. First,

$$\frac{\partial \mathcal{L}'}{\partial q_{11}} = \frac{f_{11}}{q_{11}} - \frac{v_{11}}{1-q_{11}} + \frac{M_9 q_{22}(1-q_{12}q_{21})}{q_{11}q_{22} + q_{12}q_{21} - q_{11}q_{12}q_{21}q_{22}}. \tag{33}$$

Then,

$$\begin{aligned} \frac{\partial^2 \mathcal{L}'}{\partial q_{11}^2} = &- \frac{f_{11}}{q_{11}^2} - \frac{v_{11}}{(1-q_{11})^2} \\ &- \left(\frac{M_9 q_{22}(1-q_{12}q_{21})}{q_{11}q_{22} + q_{12}q_{21} - q_{11}q_{12}q_{21}q_{22}} \right)^2. \end{aligned} \tag{34}$$

Since $M_0, \ldots, M_9$ are multinomial random variables, $\mathbb{E}[M_i] = Tr_i$. Thus, taking the negative expectation of (34) and simplifying gives

$$\begin{aligned} \mathcal{I}_{11} = &\frac{(1-q_{22})(1-q_{12}q_{21})}{q_{11}} + \frac{(1-q_{12}q_{21})}{1-q_{11}} \\ &+ \frac{q_{22}^2(1-q_{12}q_{21})^2}{q_{11}q_{22} + q_{12}q_{21} - q_{11}q_{12}q_{21}q_{22}}. \end{aligned} \tag{35a}$$

Following a similar procedure, the remaining entries of the first row are

$$\mathcal{I}_{12} = \frac{q_{21}q_{22}}{q_{11}q_{22} + q_{12}q_{21} - q_{11}q_{12}q_{21}q_{22}}, \tag{35b}$$

$$\mathcal{I}_{13} = \frac{q_{12}q_{22}}{q_{11}q_{22} + q_{12}q_{21} - q_{11}q_{12}q_{21}q_{22}}, \tag{35c}$$

$$\mathcal{I}_{14} = \frac{q_{12}q_{21}(q_{12}q_{21} - 1)}{q_{11}q_{22} + q_{12}q_{21} - q_{11}q_{12}q_{21}q_{22}}. \tag{35d}$$

Similar expressions are derived for all the entries in the Fisher information matrix.

The CRB curve in Fig. 7 is obtained using the mean of the diagonal elements of $\mathcal{I}^{-1}$. This curve and the MSEs of the estimators depend on the chosen ground truth Λ. We illustrate this with three additional examples beyond the case shown in Fig. 7. When the ground truth has high flux at only two pixels, the 2-photon estimator matches the CRB closely across the range of PPF values studied as seen in Fig. 10 (middle). This ground truth would mean that most ambiguous readouts arise from two-photon events. Thus, a 2-photon estimator reconstruction should closely match the ground truth. However, when the ground truth has high flux at three pixels as in Fig. 10 (right), this model misattributes photon counts to just two pixels (due to the rejection of three- and four-photon terms in (13)) resulting in a biased reconstruction.

5. Additional Comparisons

Here, we compare the performance of the ME with three additional baselines. The randomized assignments method is a modification of the NE where instead of imputing photon counts to *every* candidate pixel where photon incidence could have occurred, the estimator randomly picks one solution from the set of possible photon incidence locations. This leads to a decrease in the bias of the NE, as seen in the increase in PSNR in Fig. 11.

Multiphoton events occurring along the same row or same column are unambiguous as noted in Sec. 3. We can define a multiphoton unambiguous estimator that improves upon the SPE by discarding only ambiguous multiphoton events. Since this estimator uses more of the measured data and is unbiased, we expect its variance to be lower than the SPE. This is reflected in the increased PSNR value of reconstructions shown in Fig. 11.

Finally, we provide comparisons against a full readout which is free from ambiguities. We expect this model to only contain Poisson noise and hence have the best reconstruction among the methods we compare.

It can be seen that across the baselines considered, our multiphoton estimator achieves the highest reconstruction PSNR.

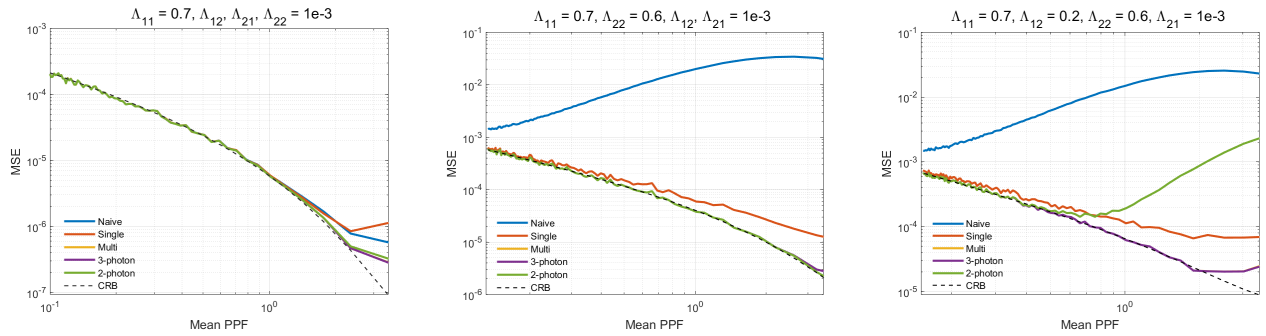

Figure 10. Dependence of estimator performance on the ground truth image. The 4-photon estimator closely matches the 3-photon estimator in these cases.

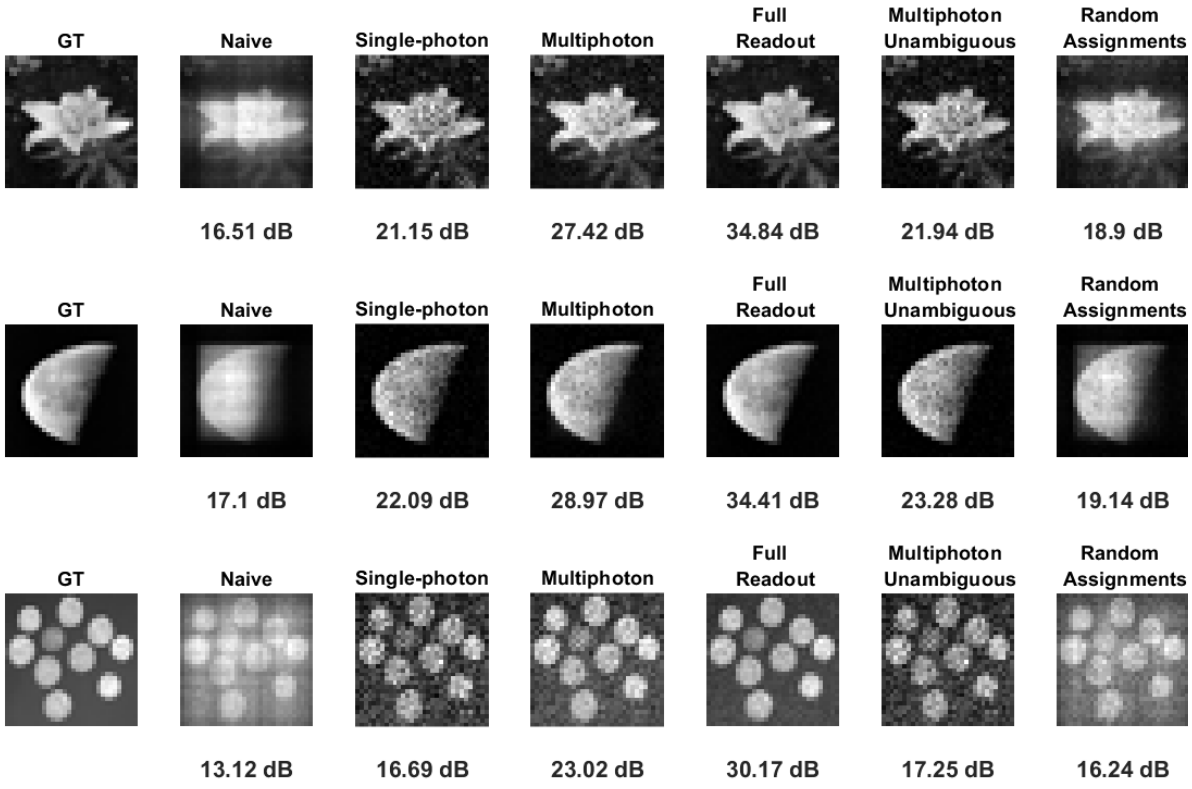

Figure 11. Comparison of the NE, SPE, and ME with full readout, multiphoton unambiguous estimator, and random assignments method.